ISSN: 2834-4928

Research Article

Journal of Electrical Electronics Engineering

# An Investigation into the Origins of Pulse-Induced Energy Gains in Electrochemical Systems

**Julian Andrew Perry***

*Kerrowenergetics.org.uk, Cornwall, UK*

***Corresponding Author**
Julian Perry, Kerrowenergetics.org.uk, Cornwall, UK.

**Submitted:** 2024, Dec 05; **Accepted:** 2025, Jan 10; **Published:** 2025, Jan 27

**Citation:** Perry, J. A. (2025). An Investigation into the Origins of Pulse-Induced Energy Gains in Electrochemical Systems. *J Electrical Electron Eng, 4*(1), 01-16.

## Abstract

*In a earlier study, inductive pulse charging (IPC), using solenoid generated high voltage transients, also known as flyback or kickback pulses, have been shown to induce energy gains in Lead acid and $LiFePO_4$ batteries, when using specific operational parameters, but with no clear indication as to the source of the additional energy. While there are presently no widely accepted theories or models regarding the energetic pathways and processes involved, it is proposed that there are only two viable possibilities for the source of the observed energy gains, as distinct from the actual mechanisms involved. The energy influx either derives from an internal response of the electrochemistry to high voltage electrostatic pulses, whereby enthalpic energy is released from the electrochemistry and serves as a form of 'fuel', or the energy influx derives from the local environment by as yet unrecognised processes and pathways. Here the battery is considered to function as part of a thermodynamically open system in the presence of 'far from equilibrium' events, such as those triggered by high voltage pulses.*

*This follow-up study, undertaken again within the Open Science Framework (OSF), sets out to test the proposed hypothesis, that internal enthalpy is the source of any pulse-induced energy influx, by looking at evidence from three main areas. Firstly, the effect of pulses on capacitors, they being devoid of any functional electrochemistry, secondly, through thermodynamic analysis and bench testing of battery capacities in conjunction with a 'chemical deficit model', and thirdly, by looking at records of battery pulse and cyclic histories to identify any long-term effects on capacity. The results, in particular the correlation between predicted and measured battery capacities with both cell chemistries, together with their pulse histories, have clearly shown that the null hypothesis of an enthalpy source must be rejected in favour of the alternative, an external source and where the battery and the local environment comprise a thermodynamically open system.*

*Consideration is also given to the possible implications of these findings for classical and quantum electrodynamic theory and how the integration of 'non-linear' and 'far from equilibrium' states might be seen as further evidence of the need for an extended and more complete model that includes interaction with the environment and otherwise anomalous phenomena.*

**Keywords:** HV Transients, Flyback Pulses, Open Thermodynamics, Battery Capacity, Electrodynamics

## 1. Introduction

Inductive Pulse Charging (IPC) uses inductively generated reverse EMF (flyback or kickback) pulses that are delivered to an electrochemical system, normally a battery. Such a device is based on a long history of related systems, derived originally from the work and observations of Daniel Cook, Nikola Tesla in the late nineteenth century, who coined the term 'radiant' effects, and further developed by such pioneers as Carlos Benitez in the early 1900s, Robert Adams, Kromrey in the 1960s, Edwin Gray in the 1970's, John Bedini, Peter Lindemann in 1960-80s, and Murakami and others into the 21st century [1-9]. Development continues to the present day but mostly falls outside of regular peer review and mainstream publications due to the unconventional, and so far unexplained, nature of the results. However, there have been various experimental generator designs proposing, for example, the use of AI and the 'Internet of Things' based control systems, or seeking to optimise the original design parameters used by their predecessors [9-13].

The results obtained from Coefficient of Performance (CoP) measurements in the first OSF study[1] with a Pulsed Flyback



[1]*The first OSF project is at: osf.io/ZTFUB*

Generator, using the phenomenon of IPC, indicate that a real energy gain is taking place in batteries subjected to inductively generated HV pulses [14]. While such pulses are often generated as part of the function of a DC pulsed motor, whereby permanent magnets in the rotor and stator assemblies serve as triggers for the switching of coils to generate the flyback pulses, a more flexible and effective method has been to decouple the pulse generation from the motor functions and to trigger the ferrite cored coils (solenoids) with a pulse width modulation (PWM) unit. This allows for precise optimisation of the pulse repetition frequency (PRF) and the switching duty cycle for a specific battery capacity and chemistry, and which also facilitates more precise control of the input energy supply. This choice does not preclude motor based systems from delivering similar types of results but rather the control of various operational parameters is more easily managed.

While the pulse generating device itself displays a typically low efficiency, in accordance with standard electrical losses, the battery plays the major role in producing the energy gains and a Coefficient of Performance CoP >> 1. The fundamental and crucial question then remains regarding the source of these measured energy gains. The situation is apparently a binary one with only two reasonable and distinct possibilities for the source of the energy. Either it arises from within the battery itself, from its internal enthalpy, or from outside of it, from the local environment and beyond. If the former, then the battery's own electrochemistry is being used and consumed in some fashion to provide the energy, possibly from the breakdown of chemical bonds and the release of chemical energy in response to the pulse charging with high voltage inductively generated transients. If instead the energy derives from outside the battery, then the electrochemistry is instead playing an intermediary role in the energy pathway, possibly serving to provide a transfer mechanism, or supporting the conditions for a 'violation' of certain aspects and interpretations of the 2nd Law of Thermodynamics [15]. Since energy is considered to enter the system across the system boundary, there is no conflict with the 1st Law of Thermodynamics, that of energy conservation, as with any thermodynamically open system such as a heat pump.

The results from charging capacitors, as described in section 2, instead of a Lead acid (Pb-A) or Lithium Iron Phosphate (LFP) battery, suggest that indeed the battery and its electrochemistry have a central role to play in the overall performance, especially since the pulse generating device itself exhibits an efficiency as low as 25 - 40%, similar to an internal combustion engine [16].

However, there are several a priori reasons why the energy gains are unlikely to derive primarily from enthalpy, by whatever route that might occur. Firstly, due to the low source impedances of the coil and the battery, once the voltage spikes reach the positive cathode terminal of the battery, they are effectively grounded in the low impedance environment and therefore would be expected to be unable to effect any significant change within the electrochemistry, such as bond dissociation and ionisation. As such, any measured energy gains must be due to other processes not yet described by conventional electrodynamics.

The second reason is that, within the electrochemistry, there are no obvious candidates amongst the active ions that are amenable to ionisation, or other energetic processes, under the influence of high voltage transients in the instances where such voltages might be sustained. Should ionisation or bond disruption occur, over the duration of the delay between absorption and re-emission, the energy released would equal the energy absorbed and so provide no net energy gain. Similarly, the conversion of one ionic species into another, via a redox reaction, would be short lived in the highly oxidising environment of the electrolyte. Again, any enthalpy changes would normally be time averaged to zero [16].

Instead, other proposed pathways suggest that the battery chemistry is acting to facilitate the influx of energy from an external and local source through the interaction of electrostatic, or other types of fields, with the chemical ions through a buffering and 'inertial' action. As such it is behaving as an open system described by the appropriate thermodynamics. The notion of open thermodynamics has been proposed for more than three decades, and with the use of various 'new' forms of language and description in an attempt to provide a rational working framework. As an open system, the unidirectional pulses are considered to introduce a high degree of recurring asymmetry across the boundary with the local environment. Here the battery chemistry acts more like a form of 'diode' to prevent the energy influx from rebalancing and regaining equilibrium, and therefore enabling it to be captured and utilised within the battery via the liberation of charge. However, the exact nature of the energy influx is unclear as, in all observations that are at first unexplained, the gathering of repeatable observations and measurable data is paramount before attempting to construct a theory to explain them.

The topic of open thermodynamics goes hand in hand with another potentially fruitful area of enquiry with regard to IPC, that of extended electrodynamics (EED). Despite the enormous success of classical electrodynamics (CED) and its quantum electrodynamics derivative (QED), where experimental proof has shown it to be the most successful theoretical model in the history of science in its descriptions of the interactions of light with matter, there are still areas of disagreement between the two. These can be resolved through EED and which leave the classical descriptions of Maxwell's electric and magnetic fields and wave equations in place, while re-introducing certain scalar and longitudinal terms that were historically removed (gauged) for mathematical convenience in the light of experimental evidence for the existence of transverse Hertzian waves available in the late 19th century [17-21].

Maxwell's original quaternion formulations theoretically postulated and demonstrated the existence of both transverse EM waves as well as longitudinal and scalar waves. After Hertz's experimental verification of the existence of transverse electromagnetic waves (TEM), Heaviside and Gibbs modified Maxwell's equations to a more convenient form that removed the longitudinal and scalar components using the Lorenz gauge which made it easier to derive solutions to the wave equations

[21]. It is these additional components, for which there is now a growing body of experimental evidence for the transmission of energy and information [20, 22-24] that may provide insights into the energetic exchanges involved in IPC and other far from equilibrium electronic states.

The rationale for determining which of the two scenarios is the most likely is described in depth in a pre- print document entitled 'Measuring Battery Health: Secondary Cell Dynamics and Electrochemistry'[2] which sets out a theoretical framework for battery health and an experimental rationale to address this question. Equally, it proposes a set of experimental techniques that can be readily undertaken to determine the status of a battery without involving the very lengthy process of measuring battery performance throughout the whole of its normal lifespan; potentially years. Therefore, a battery's status and health can be used to clarify if the battery's electrochemistry is part of the net energy gains or, alternatively, that this is not the case and therefore that some other energetic process is involved, one that nevertheless includes the electrochemistry as part of an energetic process and pathway.

The aim of this project[3] then is to determine if the proposed null hypothesis is true and that the origin of the energy gains is internal enthalpy and which implies a direct relationship between a predicted capacity, calculated from the energy released during IPC, and the actual measured battery capacity. The alternate hypothesis is that there is no relationship between the predicted and measured capacity values, and therefore that the energy gains are derived from the only reasonable alternative, the local environment of the battery.

This investigation utilises three distinct approaches. Firstly, looking at the response of a capacitor to HV transients, in the absence of any regular electrochemistry, is described in section 2. This is followed by an analysis of the thermodynamics of the different battery chemistries along with a methodology for a comparison between the calculated predicted charge capacities, using a 'chemical deficit model', and measured values. This is broken down into the thermodynamics and electrochemistry of the two battery types in section 3, a description of the 'chemical deficit model' in section 4, the experimental measurement process in section 5, the predicted and measured capacity data in section 6, the statistical methodology in section 7 and the statistical analysis and interpretation in section 8. Thirdly, an assessment of the cumulative effects of pulse and cyclic activity, using detailed historical records for the individual batteries, is in section 9. The discussion and conclusions follow in sections 10 and 11.

## 2. Capacitor Charging

Charging tests using capacitors have been undertaken throughout the exploratory phases of IPC and provide a useful comparison to those effects observed in secondary cells. Since capacitors store their energy entirely as an electrostatic field and in the absence of any electrochemistry, at first glance it would seem to offer a quick method to determine if the source of any energy gain is electrochemically dependant or not. However, this makes the a priori assumption that the only possible role for a battery's electrochemistry is as a 'fuel' source whereas it may instead serve as a channel or conduit for an energetic exchange and process. Results from IPC used with capacitors must therefore be interpreted in a wider context and not used in isolation. Further, tests with capacitors serve not only to address the question of the source of energy gains but also in measuring the internal efficiency of the pulse generation process, a value that plays an important role in the calculation of predicted battery capacity to be used with the chemical deficit model described later.

More recent tests have investigated further the effect of the pulse repetition frequency (PRF) upon the energy absorbed by a capacitor. Just as each battery was found to have an optimum PRF for the highest response, or even several over a frequency range, it was reasoned that this might also apply to capacitors. This would therefore provide a more accurate and relevant assessment in relation to any comparisons drawn with secondary cells in potentially utilising their various electrochemical processes.

To investigate the charging a capacitor, **Figure 1**[4] shows the essential elements of the pulse circuit (A), here outputting pulses to a 53mF capacitor instead of a battery, alongside a Spice simulation circuit used for theoretical comparisons (B).

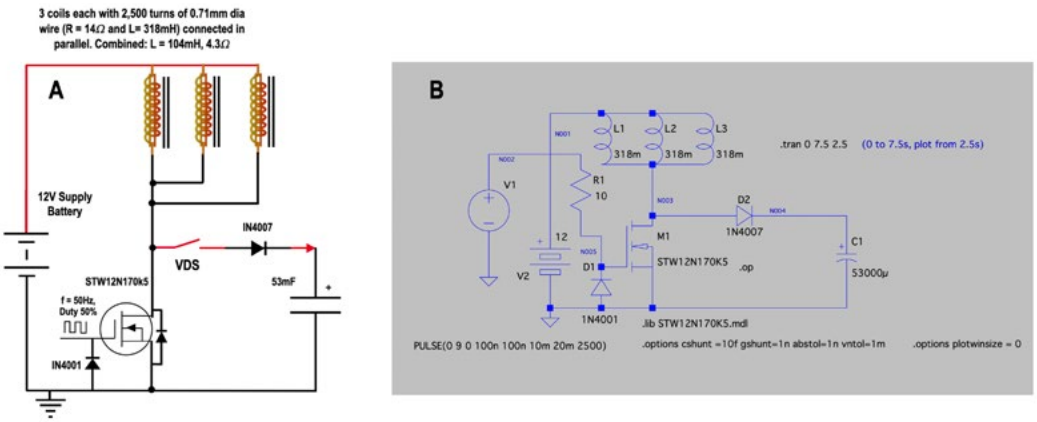


**Figure 1:** A) Essential capacitor charging schematic and B) LTSpice simulation circuit



[2]*Available at osf.io/7jhqt*
[3]*This second study and all the related files and data are available at: osf.io/BPXG6*
[4]*Full sized figures are available at https://osf.io/txy7h/*

Finding the optimum PRF was achieved using a capacitive discharge ('cap dump') unit built into the system as a high-sided voltage-dependent switch (VDS) as in **Figure 1A.** This releases the charge in the capacitor at a user set voltage as a high current pulse of typically 100A. While this has been used to observe the direct effects of such pulses on Pb-A cells, its purpose here is to allow the scoping of repetitive charging cycles so that the Vmin and Vmax and the capacitor discharge frequency (CDF) can be easily measured. The optimum PRF for the capacitor was when the CDF was at its highest value and the energy stored in the capacitor was then be derived from calculation using 1/2 $C(dV)^2$. This value was also compared with that derived from the Spice simulation circuit, (Figure 1B) where the efficiency can be derived from the ratio of the capacitor input power to the battery supply power as in **Figure 2.**

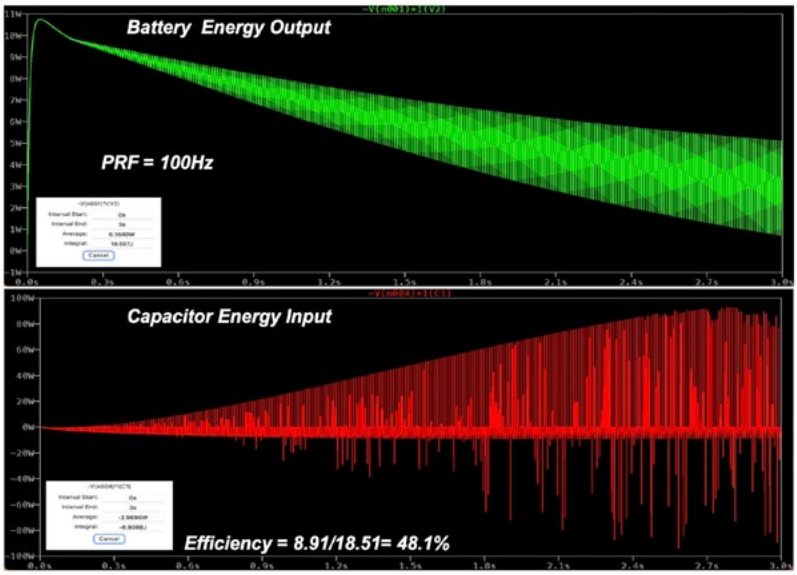


**Figure 2:** Simulator derived capacitor efficiency value at a PRF of 100Hz

In tests, the optimum PRF with the 53mF capacitor bank was found to be 40Hz in contrast to the simulation where the effect of changing frequency was driven by the accuracy of the models used. Using the capacitive discharge system, the resulting scope trace showed Vmin and Vmax, and the period of the charging T, equal to the reciprocal of the capacitor discharge frequency (CDF), allows a straightforward calculation of the energy stored in the capacitor and which can be compared to the energy supplied during the charging phase of a cycle. **Table 1** presents an example of these values and with a derived efficiency $\eta$ of 42%. Since various PRFs were used during IPC tests, up to 155Hz, depending upon the type of battery, a mean value of 34% was later used in calculating the 'energy influx'.

| Cap (mF) | $V_{min}$ | $V_{max}$ | dV | T (s)[1] | $E_{cap}$ (J)[2] | $E_{in}$ (J) [3] | $\eta$ [4] |
|---|---|---|---|---|---|---|---|
| 53.0 | 18.9 | 25.7 | 6.8 | 1.08 | 1.23 | 2.93 | 0.42 |

[1] Charging period [2] Calculated as 1/2 $C(dV)^2$ [3] Energy supplied calculated as V.I.t [4] Efficiency

**Table 1:** Capacitor charging readings and efficiency derivation

## 3. Battery Thermodynamics

The reversible redox reactions that take place in a secondary cell, such as the Pb-A variety, are the driving force for the standard electrode potentials. The changes in Gibbs energy that take place during the reactions equate to a measure of electrical work done in moving electrical charges from one electrode to the other. These various processes are explored for both Pb-A and LFP batteries.

### 3.1 Lead-Acid (Pb-A)

The electrochemical reactions for a Pb-A battery, and the half-equations taking place at each electrode, are shown in Figure 3. From standard thermodynamic theory [25], *Eqn. 1* shows that the change in internal energy U during the discharge reaction equates to the sum of the internal heat (q), expansion work (pv) and electrical work (ele).

$$\Delta U = q + Wpv + W_{ele} \qquad Eqn.1$$

For a chemical process at a constant temperature, it can be shown that q and $W_{pv} = 0$ and so the change in Gibbs energy equates solely to the electrical work done and which can also be shown to equate to the number of moles of electrons ($n_e$) x the Faraday constant (the combined charge of one mole of electrons) x $E_0$ cell the voltage across which the charges were transferred. This results in *Eqn. 2*

such that one can equate the change in Gibbs energy in the reaction to the standard cell potential where n and F are constants.

$$\Delta G^{\Theta} = W_{ele} = -n\ F\ E^{0}_{cell} \qquad Eqn.2$$

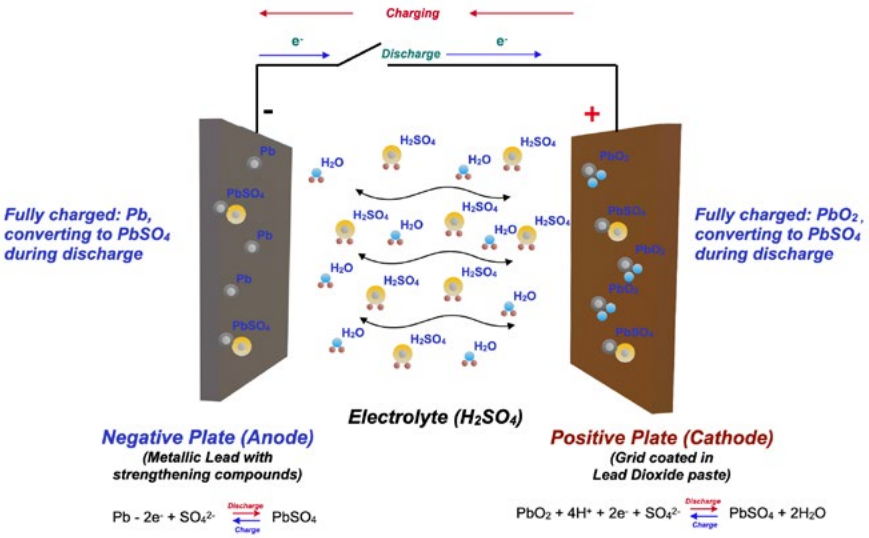


**Figure 3:** Redox reactions in lead acid batteries (derived from [25])

The general form of a reversible reaction may be described as:

$$\alpha A + \beta B \rightleftharpoons \gamma C + \delta D \qquad Eqn.\ 3$$

From this reaction the Gibbs energy of the reaction can be calculated from the sum of the Gibbs energy of the products (C + D) minus the sum of the Gibbs energy of the reactants (A + B) as in *Eqn. 3*. Therefore, using the standard thermodynamics for the reversible reactions of a secondary cell, the electrochemical potentials and the Gibbs energies involved can be derived from the charging and discharging phases of a battery's activity as in Eqn. 4.

$$\Delta_r G^{\Theta} = (\gamma \Delta_f G^{\Theta}_C + \delta \Delta_f G^{\Theta}_D) - (\alpha \Delta_f G^{\Theta}_A + \beta \Delta_f G^{\Theta}_B) \qquad Eqn.4$$

For a Lead-Acid battery, the combined chemical reaction is:

$$Pb_{(s)} + PbO_{2(s)} + 4H^{+}_{(aq)} + 2SO^{2-}_{4(aq)} \leftrightarrows 2PbSO_{4(s)} + 2H_2O_{(l)}\ (n = v_e = 2) \qquad Eqn.5$$

The combined formation energies for the Lead acid battery reactions as per Eqn. 4 are:

$$\Delta_r G\Theta = -307.6 - (-89) = -396.6k\ J/mol$$

Using: $E^{0} = \Delta G\Theta / -n\ F$ (from Eqn.2)

$$\therefore E^{0}_{cell} = -393.6kJ/mol\ /\ (-2 \times 96{,}485C/mol) = 2.06V$$

The specific charge density in Ah/g is derived from the Faraday constant and the sum of the molar masses of the reactants as in Eqn. 6:

$$q = ZF \div \sum_i M_i \text{ (where z=1)} \qquad Eqn.\ 6$$

with reference to the chemical equation (*Eqn. 5*) this gives:

$$\sum iMi = 1 \times M(Pb) + (1 \times M(PbO_2)) + (4 \times M(H)) + (2 \times (SO_4)$$

= (207.2) + (239.2) + (4) + (192.2) = 642.6g /mol

Therefore $q$ = 2 x 26.8 / 642.6 = 0.0834 Ah/g = 83.4 Ah/kg.

The specific energy density in Wh/kg is then derived from:

$$E = q\ E^{0}_{cell} \qquad Eqn.7$$

To give the Theoretical Specific Energy Density (TSED) = E = 83.4 × 2.06 = 171.8Wh/kg

### 3.2 Lithium Iron Phosphate (LFP)

Looking at an LFP battery, also used in this study, **Figure 4** shows the reversible reactions and the electrode composition. Due to the variable manner in which Li+ ions intercalate into the cathode, it is more straightforward to determine the specific charge density by using the chemical reaction, as before, and then using the observed and agreed standard cell voltage to determine the specific energy density instead of deriving the cell voltage from the formation energy.

The overall Lithium based reversible reaction is:

$$LiFePO_4 + 6C \leftrightarrows Li_{(1-x)}FePO_4 + LixC_6 \text{ (where } x \text{ is a variable factor for the intercalation)} \qquad Eqn.\ 8$$

Using the molar masses of the reactants: $LiFePO_4 + 6C$

$\sum iMi = 1 \times M(LiFePO_4) + (6 \times M(C)) = (157.8) + (72.0) =$ 229.8g /mol

Theoretical Specific Charge Density = $q = ZF \div \sum_i M_i$ = 1 x 26.8 / 229.8 = 0.117 Ah/g = 117 Ah/kg

Theoretical Specific Energy Density= $E = q\ E^0_{cell}$ = 117 x 3.45 = 403.7 Wh/kg.

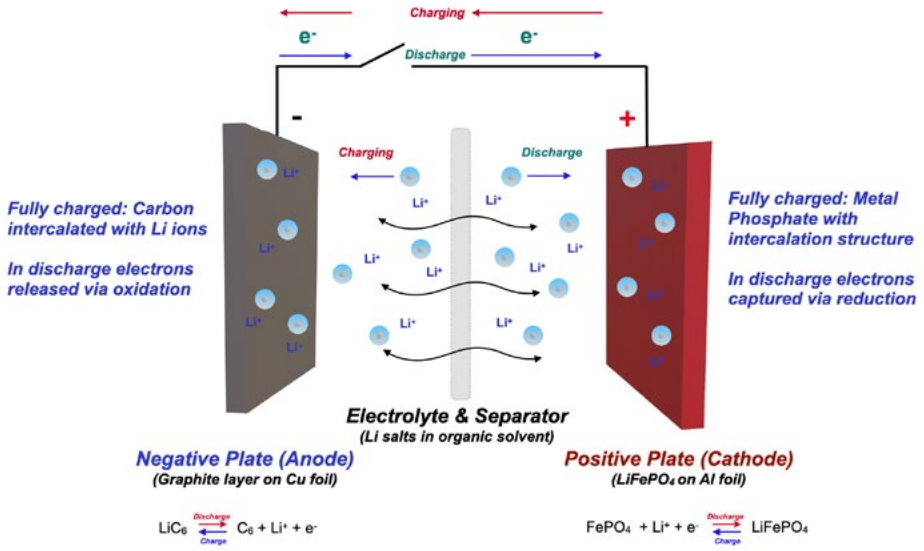


**Figure 4:** Reversible reactions and ion movements in a $LiFePO_4$ battery (derived from [26])

In practice, the actual working values for specific charge and energy capacity are much smaller than the thermodynamically calculated theoretical values, but they illustrate the much higher energy and charge densities of Lithium batteries.

With the standard thermodynamics of these secondary cells described above, the null hypothesis being tested is that the energy gains observed using IPC arise from the interaction of the HV pulses with the electrochemistry. This hypothesis therefore proposes that some of the chemical energy contained in the various bond energies is transferred to the mobile charge carriers within the electrolyte that is subsequently stored in the battery chemistry in the usual manner and with excess energy released to provide the energy gains observed in IPC. The working model for this process, and which allows for the calculation of the change in charge capacity ΔAh as a result of the release of a measurable amount of energy in IPC, is called the 'Chemical Deficit Model'. This is in contrast to the alternative hypothesis, that the energy derives from the local environment, acting in some currently unknown manner as part of an open system in conjunction with the battery's electrochemistry.

## 4. Chemical Deficit Model

The thermodynamics of the reversible reactions taking place in a battery is the basis of the chemical deficit model in that the formation energy ΔGΘ is proportional to the total charge transferred in the reaction as expressed in $\Delta G^{\Theta} = -\ n\ F\ E^0_{cell}$ (*Eqn. 2*) [25] and therefore the ratio of the charge transferred between the electrodes to the Gibbs (enthalpic) energy is simply the reciprocal of the standard cell voltage $-n\ F/\Delta G^{\Theta} = 1/E^0_{cell}$. Using this factor we can derive the change in battery charge capacity ΔAh from the energy released in Wh should ΔGΘ be the source of the energy gains.

The model therefore assumes that the pulses cause the release of all or part of the chemical bond energy in a non- reversible manner such that the active chemical agents involved will then no longer be able to participat in the normal electrochemical reversible reactions. This will result in a gradual and predictable decline in the battery's capacity and, with each session of energy release from IPC, the total battery capacity will reduce in accordance with a predicted loss of capacity ΔAh.

However, since the factor $1/E^0_{cell}$ is crucial in deriving changes to battery capacity as a function of the energy released in response to IPC, it will also be derived from first principles in a series of steps involving thermodynamic analysis and quantitative chemistry. These steps are as follows:

1. Using the molar masses involved in the electrochemical reaction equation for a specific type of chemistry (*Eqn. 6*), the 'Theoretical Specific Charge Density' (TSCD= q) in Ah/kg is calculated and, from this, using *Eqn. 7*, the 'Theoretical Specific Energy Density' (TSED=E ) is derived in Wh/kg.

2. For a particular battery with a known chemical composition, the 'Theoretical Battery Capacity' (TBC) is calculated using the TSCD value in (1) and the actual mass of its electrochemical agents. Practically, the actual 'Working Battery Capacity' (WBC) in Ah is much lower than the theoretical value due to inefficiencies within the battery and a value for WBC, as a percentage of the TBC, is obtained from practical discharge measurements to a consistent Depth of Discharge (DoD).

3. Using the percentage from the discharge measurements, a value for the 'Working Specific Charge Density' (WSCD) in Ah/kg,

is then derived from the 'Theoretical Specific Charge Density' (TSCD) and similarly a value for the 'Working Specific Energy Density' (WSED) in Wh/kg from the 'Theoretical Specific Energy Density' value (TSED). This allows for the calculation of the actual mass of active agents required to release 1Wh (3.6kJ) of energy in this particular battery.

4. Finally, the ratio of WSCD / WSED [(Ah/kg) / (Wh/kg)] = (Ah/Wh) gives a value for the change in battery charge capacity ΔAh for every Wh of enthalpic energy released from the electrochemistry.

Besides being able to predict the change in battery capacity $\Delta A$ from the release of 1Wh (3.6kJ) of chemical energy, if required we can also derive the actual mass of electrochemical agents in a specific battery required to release this energy. These steps will be laid out for the Pb-A case and the figures presented for the LFP battery.

### 4.1 Pb-Acid Example

A specific example using these steps is given for a 110Ah Pb-Acid battery, with a total mass of 6.7kg, and with the reversible chemical reaction given in Eqn. 5 as:

**1:**

$$Pb_{(s)} + PbO_{2(s)} + 4H^{+}_{(aq)} + 2SO^{2-}_{4(aq)} \leftrightarrows 2PbSO_{4(s)} + 2H_2O_{(l)} \ (v_e = 2)$$

Using the molecular masses and Eqns. 6 and 7 the values of and are derived:

$$TSCD(q) = 2 \times 26.8 \div 642.6 = 83.4\text{Ah /kg} \qquad \textit{Eqn. 9}$$

$$TSED(E) = q \times E^{0}_{cell} = 83.4 \times 2.06 = 171.8Wh/kg \qquad \textit{Eqn. 10}$$

2: From the battery specification sheet we have the total mass of the active agents in the battery that is used with the value of to give the theoretical battery capacity (TBC) for this particular battery:

Mass %w/w: Pb: 45%, $PbO_2$: 18%, $H_2SO_4$: 14% of total mass: 6.7kg

Mass $Pb_{(s)}$ = 3.02kg, $PbO_{2\,(s)}$ = 1.21kg, $H_2SO_{4\,(l)}$ = 0.94kg
∴ total active ingredients = 5.17kg

$$\therefore TBC = q \times m = 83.4Ah/kg \times 5.17kg = 431.18Ah \qquad \textit{Eqn. 11}$$

Using discharge measurements, the actual working battery capacity (WBC) is derived as a percentage of its theoretical maximum, i.e. working capacity (WBC) / theoretical capacity (TBC).

In this case the WBC = 104Ah / 431.2Ah = 24.1% (of the theoretical capacity)

3. With this percentage, the Working Specific Charge Density (WSCD) and Working Specific Energy Density (WSED) are calculated for the specific battery from the TSCD and TSED values for Pb-A:

$$WSCD = 24.1\% \times 83.4Wh/kg = 20.1Ah/kg \qquad \textit{Eqn. 12}$$

$$WSED = 24.1\% \times 171.8Wh/kg = 41.4Wh/kg \qquad \textit{Eqn. 13}$$

Therefore, the mass of active agents required to release 1Wh (3.6kJ) of energy = 1/41.4 = 0.024kg =24g.

So if the energy source for IPC is the electrochemistry, every 1Wh of energy released would result in the 'loss' of 24g of active electrolytic agents from within the battery bulk.

4. The ratio of WSCD to WSED, which also equates to the ratio $1/E^{0}_{cell}$, provides a value of the charge capacity that equates to a measured energy released in Wh. From this ratio, expressed in Ah/Wh, we can calculate the change in charge capacity ΔAh correlated with the energy released during IPC and, if desired, the mass of active chemical agents involved in the process.

$$\therefore WSCD/WSED = 20.1/41.4 = 0.486Ah/Wh \ (= 1/E^{0}_{cell} = 1/2.06) \qquad \textit{Eqn. 14}$$

The chemical deficit model therefore predicts that for every Wh of energy released we can expect the capacity of any Pb-acid battery to reduce by 0.486Ah, as determined by the state of health (SoH) and discharge measurements of the available capacity. While the relevant electrochemical agents are still part of the battery's mass, the null hypothesis proposes that they have become thermodynamically inactive in the reversible redox processes of charging and discharging.

### 4.2 $LiFePO_4$ Example

Using the same steps with an 18Ah $LiFePO_4$ battery, with a total mass of 2.2kg and active ingredients 0.484kg:

1: $TSCD(q) = 1 \times 26.8 \div 229.8 = 0.1166Ah/g = 117Ah/kg$

$$TSED(E) = q \times E^{0}_{cell} = 117 \times 3.45 = 403.6Wh/kg$$

2: TBC = 117Ah /kg × 0.484kg = 56.6Ah and a measured WBC = 16.5Ah (29.2 % of TBC )

3: $WSCD = 29.2\% \times 117Wh/kg = 34.2Ah/kg$ *and*

$$WSED = 29.2\% \times 403.6Wh/kg = 117.9Wh/kg$$

Therefore, the mass of active agents required to release 1Wh (3.6kJ) of energy = 1/117.9 = 0.0085kg = 8.5g.

4: WSCD /WSED = 34.2 /117.9 = 0.290Ah /Wh ( = 1/E0 = 1/2.06) *Eqn. 15*

These calculations confirm the use of the factor as part of a repeatable method to determine if a battery's electrochemistry is the source of the observed IPC energy gains and can be undertaken at any stage in the battery's life, particularly if reference is made to a control battery of similar age but which has had no or limited

exposure to IPC. Using this model, the total estimated energy influx arising from IPC can be translated to a predicted drop in battery capacity and then correlated with measured capacity values. The practical measurement process using this model is described next before the measurement data, statistical methodology and analysis.

## 5. Measurement Process

Measuring the battery capacity and the energy released during IPC sessions requires a consistent methodology which also protects the battery from damage due to the depth of discharge used in the capacity measurement. Such a methodology allows for uncharacteristic behaviours to be observed and tested against a control discharge.

With reference to **Figure 5**, showing each full cycle over a two day period, a complete charge-discharge cycle consists of the following stages. Firstly, a full charge, using the appropriate mains charger, and then, after at least 60 minutes stabilisation, measurement of the internal resistance, state of charge (SoC), SoH and estimated discharge current (EDC) with a conductance meter. Secondly, 5% of the nominal capacity is discharged in readiness for an IPC session and where a state of 95% of the nominal capacity is used as the charging point. Thirdly, an IPC session with a determination of the CoP and uncertainty range followed by a top-up charge to return the battery to a state of full charge. Fourthly, a 'full' discharge at a C20 rate, in this case 4A, down to a consistent DoD of 11.75V under load with automatic shutoff. Avoiding regular and complete discharge down to 7 - 9V avoids unnecessary stress and permanent battery damage. After stabilisation, the discharge time, Ah and Wh dissipated are taken, along with the internal resistance, SoC, SoH and EDC values. **Figure 6** presents the various typical graphical outputs from each of the four stages of the cycle.

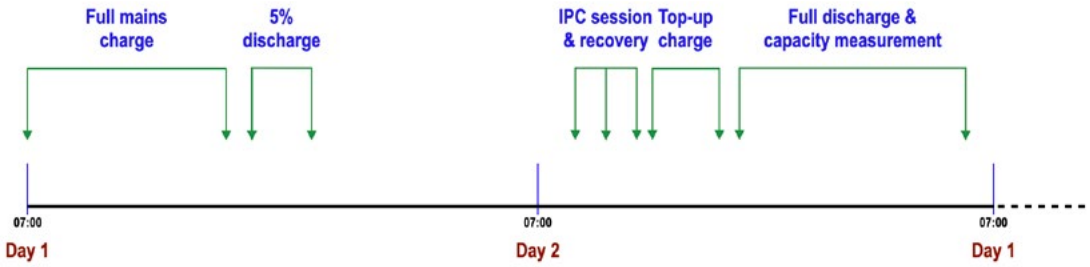


**Figure 5:** The full testing cycle sequence

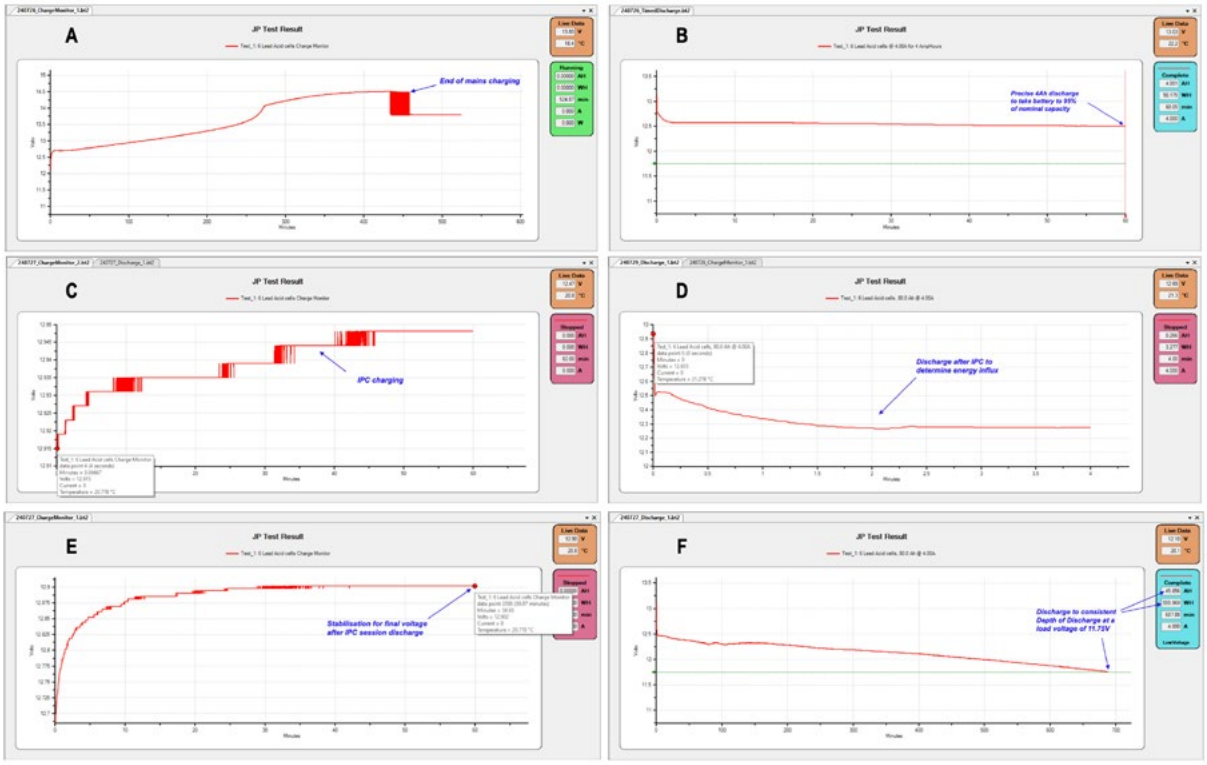


**Figure 6:** Stages of 'charge-discharge' cycle: (a) full mains charging, (b) timed 5% Ah discharge, (c) IPC charging, (d) IPC discharging, (e) IPC stabilisation and (f) full discharge-capacity measurement. (A full sized graph can be seen at: https://osf.io/gw4bk)

Once the measurements are complete then, in accordance with the chemical deficit model, the predicted drop in battery capacity is calculated using the energy released during the IPC session in conjunction with the ratio of WSCD/WSED (≡1/E0 ), and added to the data set along with the actual measured battery Cell capacity from the fourth stage (F in Figure 6).

| Test | CoP ± $\Delta_{CoP}$ | | | $E_{in}$ (kJ) | $\eta$ | Energy to CoP = 1 (kJ) | Energy to CoP value (kJ) | Total Energy Influx (kJ) | Ah/Wh | Predicted ΔAh |
|---|---|---|---|---|---|---|---|---|---|---|
| 1 | **2.59** | **±** | **0.36** | 4.15 | 0.34 | 12.21 | 6.60 | **18.80** | 0.486 | **2.54** |
| 2 | **2.06** | **±** | **0.30** | 4.18 | 0.34 | 12.29 | 4.43 | **16.72** | 0.486 | **2.26** |
| 3 | **1.96** | **±** | **0.28** | 4.18 | 0.34 | 12.29 | 4.01 | **16.31** | 0.486 | **2.20** |
| 4 | **2.78** | **±** | **0.38** | 4.22 | 0.34 | 12.41 | 7.51 | **19.92** | 0.486 | **2.69** |
| **Pb-A** | **2.45** | **±** | **0.35** | 5.98 | 0.34 | 24.79 | 8.67 | **33.46** | 0.486 | **4.52** |
| **LFP** | **8.66** | **±** | **1.31** | 1.14 | 0.34 | 3.35 | 8.73 | **12.08** | 0.290 | **0.97** |

**Table 2:** Calculation of total energy influx, and predicted ΔAh from the cop value for a Pb-A battery

To calculate the predicted capacity change, the total energy released during the IPC session is derived from the internal efficiency and the CoP value and examples are given in **Table 2**, including a typical average for both battery chemistries. First, using the measured input energy to the system, the energy required to reach a CoP = 1 is $E_{in}/\eta$. Secondly, the energy required to reach the measured CoP is $(CoP - 1) \times E_{in}$, although this component does not include the efficiency factor since the internal energetics of the influx, and how the measured efficiency relates to it, are currently unknown. For this reason the total influx is an estimated and minimum value since has not been applied to this component.

The total influx is the sum of the two components and then the $1/E^0_{cell}$ factor is applied to give a predicted value of ΔAh.

The predicted values of ΔA are then compared to those measured from discharges as shown in test figures in the next section. The two sets of values can then be assessed for any correlation, to a specified degree of confidence, using the statistical methodology described in section 7.

## 6. Predicted and Measured Capacities

Undertaking the IPC component, as depicted in stages (C) - (E) in **Figure 6**, involves the same methodology[5] used in the previous study to observe energy gains in secondary cells. The individual values of CoP are used to derive a figure for the total energy influx and then, based upon the chemical deficit model, a predicted drop in capacity is derived as in the examples in **Table 2**.

A series of 15 test cycles was conducted in accordance with the schedule shown in **Figure 5** and where **Table 4** presents a selection of data from one set of tests runs. It shows the predicted and measured values and where the differentials column (Capacity Diff.) indicates the growing difference between these two values. The smaller the differential then the more the change in capacity is in keeping with the chemical deficit model and the predicted 'loss' of active chemical agents to participate in the reversible redox reactions.

| Test No. | Bat ID | Type | Nom. Bat (Ah) | Energy released by IPC (kJ) | Predicted Capacity Loss (Ah) | Predicted Capacity (Ah) | Residual SoC | Normalised Measured Capacity (Ah) | Capacity Diff. (Ah) | Capacity Diff. (% Nom. Ah) |
|---|---|---|---|---|---|---|---|---|---|---|
| 1 | B82 | Pb | 80 | 17.17 | 2.32 | 42.3 | 27 | 48.2 | 5.91 | 7.4 |
| 2 | B82 | Pb | 80 | 18.73 | 2.53 | 39.8 | 25 | 49.8 | 10.04 | 12.5 |
| 3 | B82 | Pb | 80 | 18.33 | 2.47 | 37.3 | 24 | 49.9 | 12.61 | 15.8 |
| 4 | B82 | Pb | 80 | 16.74 | 2.26 | 35.0 | 28 | 46.7 | 11.67 | 14.6 |
| 5 | B82 | Pb | 80 | 15.34 | 2.07 | 33.0 | 32 | 44.4 | 11.45 | 14.3 |

**Table 3:** Predicted and measured capacities, and capacity differentials for the Pb-A battery (all the measurement data for both battery chemistries is available at: https://osf.io/h5gp2/)

Also recorded was the remaining SoC of the battery after each discharge at the end of each cycle. The observation that this value gradually increased promoted a need for both a normalisation of the discharge value to be undertaken and tests with a control battery, without the IPC component, to observe how it responded to sequential charge and discharge cycles. The residual SoC was

incorporated into the Ah discharge figure in each cycle by using the average SoC value of the whole set and adjusting the discharge Ah value up or down so as to reflect its final rested value. For example, if after discharge the battery remained at a higher residual SoC than the set average, then its discharge Ah was increased by the ratio of the SoC/SoC(av), and conversely with a lower residual SoC. This process produces an adjusted measured capacity value that takes into account the remaining SoC of the battery and it is these values that were used in the analysis and correlation tests.

Testing a control battery without the IPC component served to reveal inherent behaviours of the charge and discharge cycles for comparative purposes and to allow this factor to be taken into account when evaluating the effect of IPC of the cycles. For this, an identical 80Ah AGM was used and 15 identical test cycles were undertaken but without the IPC component, and similarly for the 18Ah LFP.

[5]*The 'CoP Measurement Protocol' can be seen at: https://osf.io/ygqa3/*

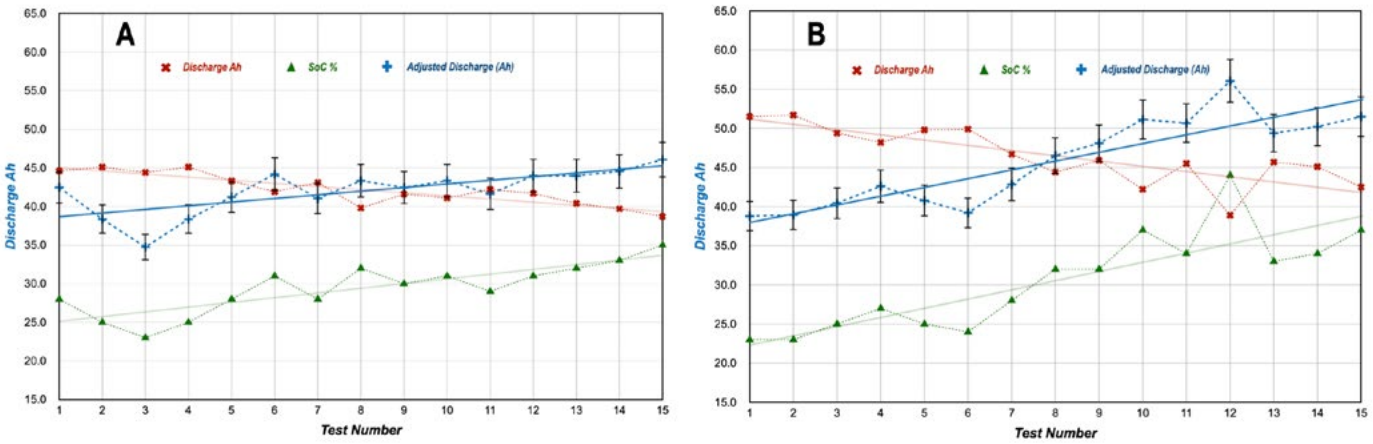


**Figure 7:** Pb-A battery (A) Control discharge capacities and (B) IPC discharge capacities. (Full sized graphs can be seen at: https://osf.io/bxzwp/)

The resulting data plots for the Pb-A battery are presented in **Figure 7** with the results for the (A) control alongside those with (B) the IPC component. For clarity, error bars are only shown for the adjusted capacity values and similarly for **Figure 8**.

Although in both parts of **Figure 7** there appears to be a gradual decline in measured Ah capacity (red line), when the residual SoC is taken into account (green line), the adjusted Ah (blue line) increases, and more so when IPC has been applied during each charge-discharge cycle **(7B)** compared to the control battery (**7A**).

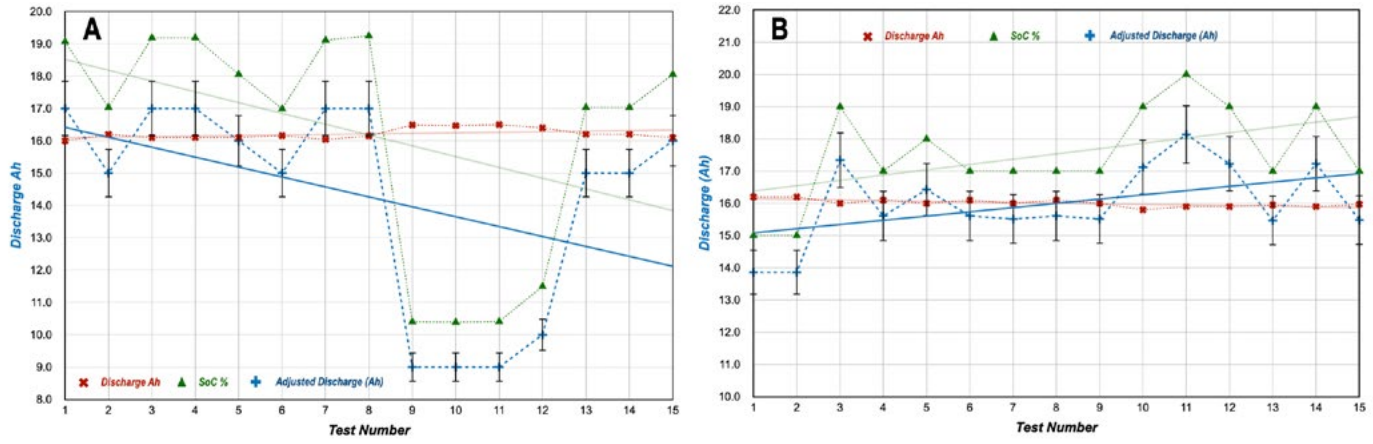


**Figure 8:** LFP battery (A) Control discharge capacities and (B) IPC discharge capacities. (Full sized graphs can be seen at: https://osf.io/zhjrw)

This suggests that another process is at work, possibly the removal of some sulphation, to offset some of the detrimental effects on the battery of normal calendric and other aging processes. For the LFP battery, the same process is presented in **Figure 8**. The large drop in the adjusted capacity values for the control LFP battery was unaccounted for in **8A** with the consistent methodology used and it contrasts with the moderate increase when IPC is used in the cycles as in **8B**.

## 7. Statistics Methodology

The statistical analysis used, to determine if the energy released during IPC derives from the 'loss' of active ingredients in the electrochemistry, requires the use of a Pearson correlation test on the predicted and measured capacity values [27]. This was done using 'R' statistical software, with a script available in the 'Analysis' component of the project files, and assumes the data are parametric and exhibit a normal distribution, and which was checked first with a Shapiro normality test [28]. Similarly, a linear regression analysis can be conducted to determine the degree of relationship between the two variables, although this is less clear since a regression line can still be drawn through a set of widely diverging capacity values with little or no correlation between them.

For both of these tests the null hypothesis is that there is a correlation and relationship between the measured and predicted capacities, meaning that the energy gains are derived from an internal enthalpic response. The alternate hypothesis is that there is no correlation between the two populations of predicted and measured battery capacity values, meaning that the energy gains arise from outside the battery and from the local environment.

With reference to **Table 3**, in the Pearson test, a coefficient $r > 0.5$ indicates a strong correlation between the two groups of data and that the two populations are linked by a causal relationship; therefore that the null hypothesis is true. This means that the energy gains derive from internal enthalpy and where the measured capacity is linked to the predicted value via the chemical deficit model. The corresponding probability (p-values) calculate the probability that the null hypothesis is true based on the data provided and is compared to the Alpha threshold measure of confidence, set at 0.05. If $p > \alpha$ then that means that the null hypothesis should be accepted and the result is not statistically significant. If on the other hand $p < \alpha$ then the p-value is statistically significant and the null hypothesis should be rejected in favour of the alternate hypothesis, that the source of the energy gains is the local environment.

| Pearson Test Values | | |
|---|---|---|
| $r > +0.5$, $p > \alpha$ | Null Hypothesis accepted | Energy gains from internal enthalpy |
| $r < +0.5$, $p < \alpha$ | Alternate Hypothesis accepted | Energy gains from local environment |

**Table 4:** Pearson correlation test threshold values

Conversely, if $r < 0.2$ then there is no significant correlation between the two populations, the measured and predicted capacity values, and therefore the alternate hypothesis is true. Should the correlation value be negative then this indicates that there is an inverse relationship of varying strength; e.g. - 0.2 weak, - 0.5 moderate and -1 very strong, in other words, as one variable becomes larger the other becomes smaller to a varying degree indicated by the correlation value, again requiring the rejection of the null hypothesis.

## 8. Statistical analysis and interpretation

The statistical methodology previously described has been applied to this data, consisting of a Pearson correlation test and a Regression plot to see if there is any relationship between the predicted and observed capacity values[6].

**Figure 9A** presents the adjusted capacity values for the Pb-A battery for both the control (blue line), IPC (red line) and for the predicted capacity (grey line) as derived from the chemical deficit model. They show the battery capacity is increasing with each test using IPC and, to a lesser extent, without IPC as in the control tests. Even if the small rise with the control tests could be accommodated with the equipment error, the IPC results are opposite and divergent to the predicted decline in capacity over time due to the proposed impact of IPC on the electrochemistry. Since the predicted values are an estimated minimum, due to the unknown effect of the measured internal efficiency on the energy influx, no error assessment has been made for these values. However, even with unknown errors in the predicted capacity values, the graphical divergence clearly indicates that the electrochemistry is not being quantitatively impacted by ongoing IPC.

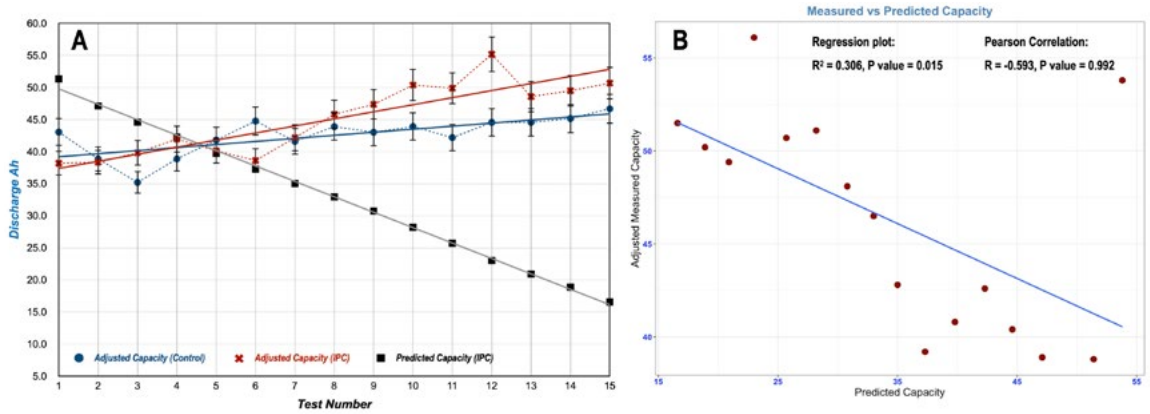


**Figure 9:** Pb-A Battery (A) Control, IPC and predicted charge capacities and (B) measured vs predicted capacities correlation plot. (Full sized graphs can be seen at: https://osf.io/a3n7w)

Looking at the regression analysis for this data in **Figure 9B**, there is a modest relationship (R2 = 0.306) between the two variables, however, contrary to expectations from the null hypothesis, the gradient shows an inverse relationship and with a negative Pearson correlation of -0.593. In other words, the capacity is not reducing in line with the chemical deficit model but is instead increasing. The gradual rise may be attributed to the effects of IPC on soft and hard sulphation thereby restoring a small proportion of lost capacity due to normal calendric aging effects.

**Figure 10** presents similarly for the LFP battery where again in **10A** there is a divergence between the measured capacity with IPC (red) and that with the control (blue) and with the predicted capacity (grey). In **Figure 10B**, there is even less of a relationship between the two values, (R2 = 0.116) than for Pb-A and again an inverse Pearson correlation (-0.419) and with a probability approaching 1.

[6]*The code used with the statistical package 'R' and the relevant exported data and plots are available in the relevant sub-components at: https://osf.io/49ch5/*

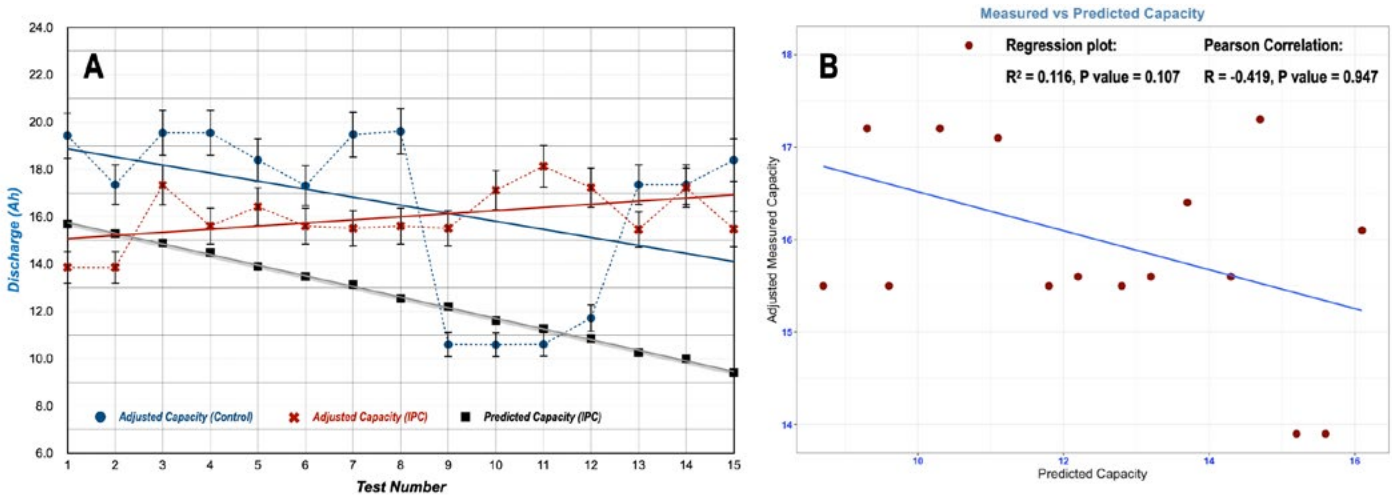


**Figure 10:** LFP Battery (A) Control, IPC and predicted charge capacities and (B) measured vs predicted capacities correlation plot. (Full sized graphs can be seen at: https://osf.io/vb8tr)

The use of a control battery, not being subjected to IPC, served to highlight any intrinsic trends in dissipated charge within the system. As indicated in Figure 7, under the same cyclic conditions, there was a slight increase in the adjusted capacity, and without any obvious mechanism for it, but the increase was larger with the use of IPC in the cycle.

In both battery chemistries, the regression plot and correlation data suggest an inverse relationship between the predicted and measured capacities, therefore supporting the rejection of the null hypothesis, i.e. that the energy arises from the local environment and not from internal enthalpy. Additionally, particularly in the case of the Pb-A battery, the use of IPC resulted in a small improvement in battery capacity, possibly due to its positive effects on the reduction of the capacity-limiting consequences of the accumulation of both hard and soft sulphation associated with calendric aging.

## 9. Battery Pulse History

The third strand of evidence arises from the historical IPC and SoH data recorded for each battery over its entire use during exploratory tests and in the two studies. **Table 7** presents this summary data for the four batteries used in the studies, including the battery age, number of IPC sessions, total pulse charging time and the minimum total energy released (Wh) as a consequence of IPC. The lower total energy released by the Pb-A battery, despite the longer pulse time, reflects the generally lower CoP values measured with this battery chemistry.

The value for the minimum total energy released (column 7 in units of MJ) was derived using the same process shown in Table 2 and compiled for every test session using IPC since the battery's acquisition. Again this value is a minimum since the efficiency value of 0.34 was only applied for part of the calculation and not beyond a CoP=1, simply because of the unknown properties and behaviour of the energetics. The energy in MJ was then converted to Wh and used with the Ah/Wh factor to give a thermodynamically equivalent value of capacity in Ah. For example, with the first entry in **Table 7** for the 80Ah AGM battery (B81), the total equivalent capacity for the minimum total energy released during its IPC history is calculated as:

| ID | Type | Nom. Cap (Ah) [1] | Age (y) [2] | Total IPC sessions [3] | Total IPC time (h) [4] | Total E disp. (MJ) [5] | Wh | Equiv. Capacity (Ah) [6] | X Nom. Capacity[7] | Present Capacity (Ah)[8] | % Nom Capacity[8] | Main Use |
|---|---|---|---|---|---|---|---|---|---|---|---|---|
| B81 | Pb-A | 80 | 7.4 | 72 | 115.7 | 2.74 | 761.2 | 369.9 | 4.6 | 48.3 | 60 | IPC & Study 2 |
| B82 | Pb-A | 80 | 0.8 | 56 | 50.3 | 1.34 | 372.3 | 180.9 | 2.3 | 56.5 | 71 | Studies 1 & 2 - IPC |
| B52 | LFP | 18 | 2.0 | 236 | 37.0 | 12.3 | 3416.9 | 990.9 | 55.1 | 15.5 | 86 | Studies 1 & 2 - IPC |
| B53 | LFP | 18 | 1.9 | 97 | 17.6 | 1.14 | 316.7 | 91.8 | 5.1 | 15.9 | 88 | IPC |
| Notes | [1] Nominal capacity [2] From purchase [3] Including swap sessions [4] Total exposure to HV pulses [5] Minimum historic energy released during IPC | | | | | | | | | | | |
| Notes | [6] Thermodynamically equivalent capacity [7] Present capacity as a % of nominal capacity. [8] Present minimum capacity and as % of nominal capacity | | | | | | | | | | | |

**Table 5:** Data summary for various batteries used in both exploratory and study tests

$$E_{total}(Wh) \times 0.486(Ah/Wh) = 761.2Wh \times 0.486(Ah/Wh) = 369.9Ah \quad Eqn.\ 16$$

This is equivalent to the capacity of approximately 4.6 whole 80Ah batteries (in the 'X Nom. Capacity' column) and yet after its 7 year history its capacity remains at approximately 60% of its original nominal capacity, with the loss mainly due to normal calendric aging processes.

Using the same approach for the LFP battery (B52), and with the thermodynamic factor of 0.29 Ah/Wh gives:

$$E_{total}(Wh) \times 0.290(Ah/Wh) = 3416.9Wh \times 0.290(Ah/Wh) = 990.9Ah \quad Eqn.\ 17$$

Here the release of a minimum of 12.6MJ equates with 55 new 18Ah batteries. In other words, to derive the total energy released during the IPC history of this particular LFP battery would require the 'conversion' of the combined electrochemistry of a minimum of 55 identical batteries. Yet measurements of the capacity of this particular battery show that it is unchanged at approximately 86% of its nominal 18Ah capacity, and set to continue at a similar level.

This data further supports the rejection of the main hypothesis in favour of the alternative hypothesis, that the energy gains are derived from the local environment and do not arise from internal enthalpy.

## 10. Discussion

The results using IPC with a capacitor indicated that the electrochemistry of a battery is central to the observed energy gains since the absence of mobile ion charge carriers in a capacitor precluded certain types of response. However, the observed CoP<1 with a capacitor does not of itself indicate that the electrochemistry is the actual source of the energy gains. While it may be convenient to see this result as a confirmation of the null hypothesis, in fact there are other possible roles that the electrochemistry might play which do not confirm it. Just as the metal spheres in between the ends of a Newton's cradle transfer momentum between the two swinging spheres at either end, it is conceivable that the electrochemistry and mobile charge carriers might provide a transfer mechanism for an energy influx, and is responsive to a particular mode or propagation of energy. As we cannot rule out an as yet unrecognised role for the electrochemistry, we are unable to use the capacitor evidence on its own to determine which hypothesis is correct. Instead, the combination of bench testing and historic records of IPC on two battery chemistries have produced a compelling case that the energy influx arises from the action of the inductively generated pulses on the system as a whole, including the local battery environment, and not its internal enthalpy.

Although this study, and the previous one [14], are only two sets of data[7], these findings have potentially far reaching implications and are supported by a wide range of related, historical and anecdotal findings. It would be easy to simply dismiss the data as anomalous and contrary to conventional theory and wisdom, but that is counter to the inductive scientific method. In this fundamental approach to scientific advancement, observations are primary and are not first filtered through current understanding before being either rejected or ignored. Instead a theoretical framework is constantly being tested for its ability to embrace new empirical evidence and where such data, that is not fully explained by a current theory, requires us to expand or adjust the theory rather than reject the data so long as it meets certain standards of quality and repeatability. The rejection threshold is therefore set by whether the evidence can persist through replication and not by how easily it slots seamlessly into an already existing theory. Accordingly, Popper's theory of falsifiability [29] proposes that every theory is only one good piece of unfitting evidence away from revision, or potentially rejection. Perhaps the more important question then is does this data meet the quality and rigorous requirements to warrant expanding electrodynamic theory, for example, or engaging with some other set of burgeoning and plausible ideas? If the answer is not yet then it may at least provide a piece of a jigsaw, contributed to by others from related disciplines, and which builds a picture of an increasing tension between the present and future states of a theoretical framework.

There are various uncertainties and unknowns in this study, the most significant being the quantification of the energy influx (**Table**



[7]*There are two currently unreported replications underway.*

**2**) due to the unknown effect of the measured pulse generating efficiency on the energy influx. However, recognising that the figures used are substantially underestimated, due to the exclusion of the pulse efficiency figure in the calculation, then the case for the rejection of the null hypothesis is in fact strengthened. One may also argue that there might be a third option for the energy source, but so far the question has been designed as a binary one with only two possibilities; inside or outside of the battery. However, it is acknowledged that, while the 'outside' option has been shown to be consistent with the data, unpicking how an apparently open system behaves in this context is another journey. If then the requirements for good repeatable evidence were to be satisfied, what sort of adjustments to relevant theory or new ideas might be appropriate to explore?

Two main areas emerge as fruitful candidates for possible IPC mechanisms that result in a CoP>1 and an energy influx from the local environment. The first is 'extended electrodynamics' (EED) and the second is open thermodynamics in the context of the vacuum and the zero point field with its associated energy[8].

Despite the huge success of classical electrodynamics (CED), and in its quantum counterpart quantum electrodynamics (QED), which describes the interactions of light and matter and which was able to explain the photoelectric effect and absorption spectroscopy which CED could not, there have been long standing arguments that CED is incomplete from both experimental and theoretical considerations [30]. Much of this debate has centred around the question of whether the electric scalar potential (Φ) and the magnetic vector potential (A) are mere mathematical entities to facilitate the computation of various solutions to Maxwell's equations, or if they have some physical significance.

However, since QED has now recognised the magnetic vector potential (A) as one of the four fundamental forces in Nature, alongside the electro-weak, the strong force and gravity, its profile has once again risen to its correct place and in the spirit of Faraday's store of 'field momentum' that can be exchanged with the kinetic energy and momentum of charged particles in a conductive medium [31]. This position has been further supported by experimental verification of the Maxwell-Lodge and the Aharonov-Bohm effects, both of which demonstrate the physical presence and interactions with the magnetic vector potential A. Reinstating the potentials into CED via EED heals the unnatural schism that has divided the classical interpretation from the quantum one [32,33].

Decades of work have gone into developing EED which has been rigorously derived from CED and without the Lorenz gauge condition being applied that precluded and masked the presence of an electroscalar wave [34,35]. Often instead denoted by the term scalar longitudinal wave (SLW), it is produced by an irrotational (curl-free) current and consists of a longitudinal electric field and a scalar component. Since the longitudinal fields $E^L$ and $J^L$ are curl-free, there is no magnetic B-field and therefore no eddy currents such that SLW are unimpeded by the frequency dependent skin effect [20] and these details give rise to various predictable consequences when using HV electrostatic pulses.

Vacuum physics has similar undergone extensive development and is considered to be critical to new developments in Physics and Cosmology to name just two [36]. However, the notion of extracting energy from the vacuum is fraught with conceptual and practical difficulties. For one, as the fundamental ground state of a physical system, the zero-point fields (ZPF) and associated zero-point energy (ZPE) are not amenable to extraction in principle due to their random nature and lowest energy state. Nevertheless, as demonstrated by the Casimir effect, the extraction of vacuum energy as heat is not only possible but does not violate the conservation of energy [37]. Similarly, temporary and local changes in the vacuum energy density and associated entropy may offer possible mechanisms for extraction [38].

Non-equilibrium states, such as those generated temporarily by HV transients and pulses, can create so called dissipative structures that function as open systems and configure the spacetime metric to achieve an energy flow [39,40]. At the moment, even with the proposal that all particles and fields can be derived from one fundamental assumption and entity, that of spacetime itself, there are various hurdles to overcome in the development of viable theories for vacuum energy extraction, even if to do so is highly motivated [41]. Nevertheless, there have been various soundly based attempts that have not yet resolved all possible alternative explanations for the positive results achieved so far and which require the extension of QED into a relatively recent development called stochastic electrodynamics (SED) [42,43].

SED provides a classical description of events that would otherwise require a quantum description and incorporates Plank's constant that is so central to the descriptions used in quantum mechanics (QM) for quantised states and the model expressed by QED. Therefore SED offers a classical theory that describes physical phenomena at all scales and includes a ZPF that is 'real' in the classical sense and been shown to provide the physical basis for equilibrium between classical charged particles and classical EM radiation such as that involved in stable atomic electron orbits [43].

Here then lies the dilemma with what may be seen as anomalous data or which sit outside of currently accepted theory. Replications and linkage to similar observations within other disciplines may eventually reach a point where such a paradigm shift becomes inevitable and the only viable and considered option. Such shifts serve as points of inflection in the evolution of science and gateways to a new level of accepted normality and where the earlier view is recognised as just one of many stepping stones.

## 11. Conclusions

The hypothesis that the observed energy gains from IPC can be explained by the release of enthalpy from a battery's electrochemistry has been shown to be false due to the lack of any correlation between thermodynamically predicted capacities



[8]*Both of these will be explored in detail in a subsequent paper.*

and measured values. This has been backed up by examining the IPC histories of a variety of batteries and the thermodynamically equivalent capacities of the total energies released. The evidence from capacitor charging is unable to contribute to this question since alternative roles for the electrochemistry cannot be ruled out besides that of being an enthalpic source of energy.

The only viable alternative hypothesis is therefore accepted, that the observed energy influx derives from the local environment and with the whole battery and pulse system behaving as an open system. This raises significant implications for the completeness of certain branches of physics regarding their ability to predict and describe data that falls outside of their present remit and to maintain the exclusion of the environment as part of a larger interactive system. In this particular domain, the fields of classic electrodynamics (CED), and its proven derivative as extended electrodynamics (EED), as well as long standing deliberations regarding the nature of the vacuum in QED and SED, provide fruitful areas of enquiry into plausible mechanisms and energetic processes for IPC and will be further explored.


## Acknowledgements

The author wishes to acknowledge the support of Dr Glenn Ramsey, Joel Perry and Rodolphe Reuchlin in proof reading this manuscript.


## References


1. Cook, D, M. (1871). Improvements in Induction Coils. US Patent 119,825A. *US Patent and Trademark Office*.
2. Tesla, N. (1893). *On light and other high frequency phenomena*. Good Press.
3. Benitez, C, F. (1918). New Process for the Generation of Electrical Energy, Patent GB121561, *UK Patent Office*.
4. Aspden, H., Adams, R, G. (1993). Electrical motor-generator, Patent GB2282708A.
5. Kromrey, R. (1968). Electric Generator, Patent US3374376A. *US Patent and Trademark Office*.
6. Gray Sr, E. V. (1985). U.S. Patent No. 4,661,747. *Washington, DC: U.S. Patent and Trademark Office*.
7. Bedini, J. C. (2001). Patent No 6,677730B2. *Washington, DC: U.S. Patent and Trademark Office*.
8. Lindemann, P., & Murakami, A. (2013). Bedini SG-The Complete Intermediate Handbook. *Washington: A & P Electronic Media Liberty Lake.*
9. Sriphan, U., Kerdchang, P., Prommas, R., & Bunnang, T. (2018). Coefficient of performance of battery running and charging by magnet generator Bedini. *Journal of Electrochemical Energy Conversion and Storage, 15*(4), 041002.
10. Chrysocheris, I., Chatzileontaris, A., Papakitsos, C., Papakitsos, E., & Laskaris, N. (2024). Pulse-Charging Techniques for Advanced Charging of Batteries. *Mediterranean Journal of Basic and Applied Sciences (MJBAS), 8*(1), 22-36.
11. Ali, A. H., & Ismail, A. N. C. (2017). Design and simulation of self-running magnetic motor. *Journal of Engineering Technology, 5*, 27-31.
12. Murad, P. A., Boardman, M. J., Brandenburg, J. E., & Mitzen, W. (2020). A Nonlinear Electromagnetic Device and Potential Explanations. *Science, 6*(12).
13. Inam, H., & Al-Turjman, F. (2021). Intelligent free energy usage through radiant energy space phenomenon: An IoT-powered prototype for modified Bedini generator. *Microprocessors and Microsystems*, 104319.
14. Perry, J.A. (2024). Pulse-Induced Energy Gains in Electrochemical Systems. *J Electrical Electron Eng, 3*(4), 01-15.
15. Sheehan, D. P. (2022). Beyond the Thermodynamic Limit: Template for Second Law Violators. *Journal of Scientific Exploration, 36*(3).
16. Perry, J. A. Measuring Battery Health-Cell dynamics and electrochemistry. OSF preprint.
17. Ohmura, T. (1956). A new formulation on the electromagnetic field. *Progress of Theoretical Physics, 16*(6), 684-685.
18. Barrett, T. W. (1993). Electromagnetic phenomena not explained by Maxwell's equations. In *Essays on the formal aspects of electromagnetic theory* (pp. 6-86).
19. Arbab, A. I., & Satti, Z. A. (2009). On the generalized Maxwell equations and their prediction of electroscalar wave. *Progress in physics, 2*(8), 8-13.
20. Hively, L. M., & Loebl, A. S. (2019). Classical and extended electrodynamics. *Physics Essays, 32*(1), 112-126.
21. Reed, D. (2019, June). Unravelling the potentials puzzle and corresponding case for the scalar longitudinal electrodynamic wave. *In Journal of Physics: Conference Series* (Vol. 1251, No. 1, p. 012043). IOP Publishing.
22. Hunt, B. J. (2012). Oliver Heaviside: A first-rate oddity. *Physics Today, 65*(11), 48-54.
23. Dollard, E. (2014). Electromagnetic Induction and its Propagation.
24. Marsh, A. (2020, August 18). Tesla Coil Geometry and Cylindrical Coil Design.
25. Schmidt-Rohr, K. (2018). How batteries store and release energy: explaining basic electrochemistry. *Journal of chemical education, 95*(10), 1801-1810.
26. Goodenough, J. B., & Park, K. S. (2013). The Li-ion rechargeable battery: a perspective. *Journal of the American Chemical Society, 135*(4), 1167-1176.
27. Turney, S. (2022). Pearson correlation coefficient (r)| guide & examples. *Retrieved from Scribbr.*
28. University of Lincoln, (2024). Shapiro-Wilk Test of Normality.
29. Popper, K. (1934). *The logic of scientific discovery. Routledge.*
30. Hively, L. M., & Giakos, G. C. (2012). Toward a more complete electrodynamic theory. *International Journal of Signal and Imaging Systems Engineering, 5*(1), 3-10.
31. Konopinski, E. J. (1978). What the electromagnetic vector potential describes. *American Journal of Physics.*
32. Hively, L. M., & Land, M. (2021, July). Extended electrodynamics and SHP theory. In *Journal of Physics: Conference Series* (Vol. 1956, No. 1, p. 012011). IOP Publishing.
33. Reed, D., & Hively, L. M. (2020). Implications of gauge-free extended electrodynamics. *Symmetry, 12*(12), 2110.
34. Faddeev, L. D., Khalfin, L. A., & Komarov, I. V. (2004). VA

Fock-selected works: *Quantum mechanics and quantum field theory*. CRC Press.
35. Woodside, D. A. (2009). Three-vector and scalar field identities and uniqueness theorems in Euclidean and Minkowski spaces. *American Journal of Physics, 77*(5), 438-446.
36. Wilczek, F. (2016). Physics in 100 years. *Physics Today, 69*(4), 32-39.
37. Puthoff, H. E. (1990). The energetic vacuum: implications for energy research. *Spec. in Sci. & Technology, 13*, 247.
38. Ford, L. H. (2010). Negative energy densities in quantum field theory. *International Journal of Modern Physics A, 25*(11), 2355-2363.
39. Tiezzi, E. B. P., Pulselli, R. M., Marchettini, N., & Tiezzi, E. (2008). Dissipative structures in nature and human systems. *Design & Nature IV: Comparing design in nature with science and engineering, Brebbia CA (ed.), WitPress, Boston*, 293-300.
40. Kondepudi, D., Kay, B., & Dixon, J. (2017). Dissipative structures, machines, and organisms: A perspective. Chaos: *An Interdisciplinary Journal of Nonlinear Science, 27*(10).
41. Macken, J. A. (2015). The universe is only spacetime. *Santa Rose California.*
42. Moddel, G., & Dmitriyeva, O. (2019). Extraction of Zero-Point Energy from the Vacuum: Assessment of Stochastic Electrodynamics-Based Approach as Compared to Other Methods. *Atoms, 7*(2), 51.
43. Cole, D. C. (2019). Energy considerations of classical electromagnetic zero-point radiation and a specific probability calculation in stochastic electrodynamics. *Atoms, 7*(2), 50.